INTRODUCTION

The problem of convergence of the two-body effective interaction expansion[1] has been extensively investigated in the last few years. Shell model calculations of the spectra of mass 18 nuclei, including terms up to 3rd order in the expansion [2-6], have been performed and no definite conclusion about the convergence of the expansion could be drawn.

Calculation including average 4th order terms[7] has also been performed and the contributions from these terms were found to be as important as 2nd and 3rd order terms. The expansion seems to be slowly convergent and it might even be only an asymptotic expansion. The most important 2nd order term is the core polarization (Fig. 1a). Addition of a two-body effective interaction, derived from the two-pion-exchange three-nucleon potential[8], to the nucleon-nucleon interaction which enters in the two-body effective interaction expansion, produces an effect[9] which is opposite to the core polarization but its size is small.

The problem of convergence seems to come from the tensor component of the nucleon-nucleon interaction which is too strong. In fact, diagrams to which the tensor component contributes exhibit slow convergence with respect to the excitation energy of the intermediate states so that states up to at least 10 $\hbar\Omega$ excitation energy must be included in the intermediate states summation ($\hbar\Omega$ is the separation energy of the harmonic oscillator levels). This is the case with the core polarisation diagram[10].

The calculation done by G.Bertsch[2] used as nucleon-nucleon interaction the Kallio-Koltveit potential and the calculation by E.A.Sanderson et al.[4] used the modified Sussex matrix elements[4] which are obtained from two nucleon experimental data. Both calculations include 2nd order terms only. The D-state probability of the deuteron, P_D, is 4% for the Sussex interaction.

The other calculations[3,5,6,7] used the Hamada-Johnston or the Reid soft core potentials as nucleon-nucleon interaction. Both potentials give $P_D \tilde{=} 6.5\%$, thus their tensor component is stronger than the tensor component of the Sussex interaction. One might then expect that this last interaction provides an effective interaction expansion with better convergence properties[4].

The Hamada-Johnston, the Reid soft core and the Sussex interactions reduce to the one-pion exchange potential for large distances and until recently were considered the best phenomenological nucleon-nucleon interactions. However, a nucleon-nucleon interaction derived from field theory has always been sought. The momentum space one-boson exchange potentials (OBEP) proposed by Holinde and Machleidt were derived from field theory and have a weak tensor component. The HM1[11] potential (which was their first version) gives $P_D=5.75\%$, while those proposed more recently[12] give smaller values for P_D. According to K.Holinde[12], P_D has to be restricted to the range 4.5-5.5%, which rules out the potentials mentioned before. The OBEP reproduce the nucleon-nucleon phase shifts better than any other existing nucleon-nucleon interaction. They therefore provide the best interaction presently known.

In this paper, a shell model calculation of spectra of mass 18 nuclei is performed using as nucleon-nucleon interaction the OBEP proposed by Holinde and Machleidt[11,12]. The effective interaction expansion for such nucleon-nucleon force stands a better chance of convergence since its tensor component is weaker than the Hamada-Johnston or Reid soft core tensor components. The calculations were done using the Brueckner reaction G-matrix bare matrix elements only and bare plus core polarisation (Fig. 1a). Comparison with results of calculations using the Reid soft core potential shows that indeed the effect of the core polarisation term is smaller for the OBEP, mainly for the low lying states of ^{18}O and ^{18}F. Nevertheless, the effect of the core polarisation term is still large. The addition of a two-body effective interaction derived from the two-pion exchange three-nucleon potential should reduce that effect[9] as already mentioned.

As is well known[3,4,5,7,10,15], the spectra are very much dependent on the energy gap, C, between the single particle energy spectrum of valence and occupied states and the single particle energy spectrum of unoccupied states which are used in the calculation of the Brueckner G-matrix. For the OBEP such dependence is smaller than for the Reid soft core or Hamada-Jonhston potentials.

The calculation of the G-matrix elements in the harmonic oscillator (H.O.) basis was done using the Barrett-Hewitt-McCarthy[13] method. A brief description of the method and of the OBEP are given in section 1. The results and discussion are presented in sections 2 and 3 respectively.

1) CALCULATIONAL PROCEDURE

The Barrett-Hwitt-McCarthy method[13] for calculating the G-matrix elements in a H.O. basis is simple and provides an exact treatment of the Pauli operator Q. In this method a reference reaction matrix, $G^R(Q=1)$, is calculated first and the G-matrix is obtained from it by matrix inversion. The expression for the G-matrix elements in terms of G^R matrix elements (in the H.O. basis) is

$$G_{\beta\alpha}(\omega) = G^R_{\beta\alpha}(\omega) - \sum_{\mu}^{\infty} G^R_{\beta\mu}(\omega) \left[\frac{1 - Q_\mu}{\omega - \varepsilon_\mu} \right] G_{\mu\alpha}(\omega) \qquad (1.1)$$

The greek indices label 2 particle H.O. states, the ε's being the H.O. two-particle energies solutions of the equation

$$H_o \, \phi_\alpha = \varepsilon_\alpha \phi_\alpha \qquad (1.2)$$

the states ϕ_α being two-particle H.O. states and H_o the 2-particle H.O. Hamiltonian.

The parameter ω in Eq.1.1 is the so called starting energy and as one can see from that expression a shift of the unoccupied single particle spectrum (relative to the valence and occupied spectrum) by an amount C can be accomplished by redefining ω as $\omega - 2C$.

The matrix elements of G^R in the H.O. basis are given by:

$$G^{R}_{\beta\alpha}(\omega) = (\varepsilon_{\alpha}-\omega) \sum_{i=1}^{\infty} \frac{E_i-\varepsilon_{\beta}}{E_i-\omega} b_{i\alpha} b_{i\beta}$$

where the energies E_i are the eigenvalues of the Schrödinger equation for two interacting particles bound in the H.O. potential H_o:

$$(H_o+V)\ \psi_i = E_i\ \psi_i \tag{1.3}$$

(V is the nucleon-nucleon potential). The coefficients $b_{i\alpha}$ are the overlaps of the eigenvectors ψ_i with the H.O. two-particle states ϕ_α (Eq.1.2):

$$b_{i\alpha} = \langle \psi_i | \phi_\alpha \rangle$$

The states ψ_i and ϕ_α can be decomposed in partial waves and the radial parts can be transformed to relative and center of mass coordinates. The coefficients $b_{i\alpha}$ can then be expressed in terms of overlaps of the radial parts of ψ_i and ϕ_α in the relative coordinate. Given these relative coordinate overlaps, the G-matrix elements (1.1) can be calculated using the computer program written by Barrett, Hewitt and McCarthy.

The OBEP are in momentum space and have the following structure:

$$V(\vec{q}\,',\vec{q}\,) \sim \sum_{\alpha} \frac{g_\alpha^2\ F_\alpha^2}{k^2-m_\alpha^2}\ ,\ \alpha = \pi,\ \eta,\ \sigma,\ \delta,\ \rho,\ \omega,\ \phi \text{ mesons},$$

where $\vec{q}$ and $\vec{q}\,'$ are the nucleon vector momenta,

$k^2 = (E_{q'}-E_q)^2 - (\vec{q}\,'-\vec{q}\,)^2$, $E_q=(M^2+q^2)^{1/2}$ (M is the nucleon mass), g_α are the coupling constants and F_α are the form factors which take into account the extended structure of the nucleon and have the following form:

$$F_\alpha = \frac{\Lambda_\alpha}{\Lambda_\alpha^2-k^2}$$

Λ_α are the cut-off parameters. A small Λ_π means a strong suppression of the one-pion exchange potential in the inner region. The HM1[11] potential has different values of Λ for different mesons and has a value of 2500 MeV for Λ_π. The potential named HM3A[12] has Λ=1530 MeV for all mesons and HM3B[12] has Λ_π=1265MeV, while for all the other mesons Λ=1530MeV.

As the OBEP are in momentum space, the Schrödinger equation (1.3) has to be written in momentum representation so that the resulting equation to be solved in the relative momentum is the integro-differential equation: (Eq.(17) of reference 14)

$$(\frac{h^2}{M}\,p^2-\kappa\frac{d^2}{dp^2}+\kappa\,\frac{\ell(\ell+1)}{p^2}-E_n)a^n_{\ell sj}(p) + \sum_{\ell'}\int_0^\infty dp'pp'V^{sjt}_{\ell\ell'}(p,p')a^n_{\ell' sj}(p') = 0$$

where $\kappa = \frac{M\Omega^2}{4}$. The coupling occurs for partial waves $^3S_1$-$^3D_1$ and $^3P_2$-$^3F_2$.

Given the eigenvectors $a^n_{\ell sj}(p)$ in relative momentum, it is very simple to calculate their overlaps with the relative momentum H.O. wave functions.

The above integro-differential equations were solved using part of a computer program written by W.Glöckle and R.Offermann[14] for solving the triton problem in momentum space.

2) NUMERICAL RESULTS

The shell model calculations of mass 18 nuclei spectra were restricted to the s-d shell and used the experimental single particle energies of ^{17}O: $\varepsilon_{0d5/2}$=0 MeV, $\varepsilon_{1s1/2}$=.87 MeV and $\varepsilon_{0d3/2}$=5.08 MeV. We used a H.O. basis with $\hbar\Omega$=14 MeV. The core polarisation term (Fig. 1a) was calculated with intermediate state excitation up to 2h only, as we are mainly interested in comparing its effect for different potentials.

In Table 1 the parameters of the HM1[11], HM3A[12] and HM3B[12] potentials are given. The deuteron data are shown in Table 2. The calculations were done for five values of the gap parameter C:50.5, 25.5, 17.5, 12.0 and 8.0 (MeV). Figures 2-5 show the low lying states of ^{18}O (T=1) as a function of the gap parameter C for Reid, HM1, HM3A and HM3B, respectively. The dashed lines correspond to the results for the bare G-matrix elements only and the full lines contain the core polarisation term ($2\hbar\Omega$ excitation intermediate states). Figures 6-9 show the same thing for ^{18}F (T=0).

The ground state of ^{18}O and ^{18}F (including the core polarisation term) for all four potentials as a function of C are shown in figures 10 and 11 respectively. The dependence of these states on the C parameter is clearly smaller for the OBEP than for the Reid potential. In particular, the HM3B potential is the one which is less dependent on C.

The dependence of the spectra on C is a well know problem. Vary and Yang (15) have made an extensive study of such dependence for a phenomenological potential and concluded that the best value in this case is C=20 MeV. Comins[12] also indicated that a relatively small C would lead to a faster

convergence in excitation energy of diagrams containing one-body potential and G-matrix insertions. The core polarisation diagram converges more rapidly for Smaller C[6]. So all indications are that a small value of C should be used. A comparison of the spectrum of ^{18}O for all the potentials with C=17.5 MeV is shown in figure 12. In figure 13, the comparison is made for ^{18}F, for the same value of C. The experimental[17] spectra are also shown for completeness as there is not much point in making a comparison with experimental results at this stage.

3) DISCUSSION OF THE RESULTS

The dependence of the spectra on the energy gap C is smaller for the OBEP as expected since they have a much weaker tensor component than the Reid potential. The HM3B potential is the one which is less dependent on C but still the dependence is not negligible for the lowest lying states.

From figures 12 and 13, one sees that the effect of the core polarisation term is smaller for the OBEP than for the Reid potential but again the effect is still rather large mainly for the lowest lying states. The main difference is for the ground states in which cases the core polarisation effect for the Reid potential is much larger than for the OBEP and the inclusion of the core polarisation term produces very similar spectra for all four potentials. Before comparison is made with experiment, one should include at least all the other 2^{nd} order terms which are shown in Fig. 1b-d. After the core polarisa-

tion term, the 4 particle-2hole (4p2h) term (Fig. 1b) is the most important of these 2^{nd} order terms and in general the other 2^{nd} order terms (Fig.1-c,d) are neglected even though they have been shown to be different from zero[4,18] (these terms would be identically zero if a self consistent single-particle basis had been used instead of the H.O. basis). The addition of the 4p2h term produces in general a lowering of the states [2,3] and the shift produced by this term is in general much smaller than the shift due to the core polarisation term.

The spectra of ^{18}O for C=12MeV are shown in figure 14. The third spectrum showns the effect of the addition, to the Reid potential, of the effective two-body interaction[9] obtained from a three-nucleon potential derived from the two-pion-exchange amplitude. The same comparison is made for ^{18}F in fig.15. From these results one can see that the addition of such two-body effective interaction will cause some suppression of the core polarisation term and the ground states are the most affected by the addition of such term.

From the present calculation, it is possible to predict that the 3^{rd} order terms effect will certainly be smaller for the OBEP than for the Reid soft core potential. These results indicate that the convergence of the effective interaction expansion is better for the OBEP but it does not seem strikingly better as 3^{rd} order terms seems to be still important and probably also 4^{th} order. The HM3B potential seems to be the best one as it exhibits smaller dependence on the gap parameter C, i.e., it has the weakest tensor component. It also gives the best triton binding energy: -8.00 MeV[19].

ACKNOWLEDGEMENTS - I would like to thank Dr. Margareth Sandel for her great help in the use of the Barrett-Hewitt-McCarthy and core polarisation codes. I am also thankfull to Dr.W.Glöckle and Dr.R.Offermann for making available to me their momentum space code.

I would like to thank the kind hospitality of the Department of Physics of the University of Arizona during my stay there.

I would like to thank particularly Dr. S.A.Coon and Dr.B.R.Barrett for discussions and help when I could not move around.

REFERENCES

(1) C.Block and J.Horowitz - NP8(1958),91
B.H.Brandow - Rev. of Mod. Phys. 39 (1967),771
B.H.Brandow - Lectures on Theoretical Phys. Vol.XIB - ed. K.T.Mahanthappa and W.E.Britten, Gordon and Breach (N.Y. 1969),55.

(2) G.F.Bertsh - N.P.74 (1965),234.

(3) T.T.S. Kuo and G.E.Brown - N.P.85 (1966),40
T.T.S.Kuo - N.P.A103 (1967),71.

(4) E.A.Sanderson, J.P.Elliott, H.A.Mavromatis and B.Singh - N.P.A219 (1974)190.

(5) B.R.Barrett and M.W.Kirson - N.P.A148(1970),145.

(6) Margareth Sandel - PhD Thesis. University of Arizona (1977)

(7) P.Goode and D.S.Koltun - N.P.A243 (1975),44.

(8) S.A.Coon, M.D.Scadron and B.R.Barrett - N.P.A242 (1975), 467.

(9) S.A.Coon, R.J.McCarthy and C.P.Malta - J.Phys.G. Nucl.Phys. 4 (1978),183.

(10) J.P.Vary, P.V.Sauer and C.W.Wong - Phys.Rev. C7 (1973),1776.

(11) K.Holinde and R.Machleidt - N.P.A247 (1975), 495; N.P.A256 (1976), 479; N.P.A256 (1976), 497.

(12) K.Holinde - "πNN form factor and two nucleon data" - to be published.

(13) B.R.Barrett, R.G.L.Hewitt and R.J.McCarthy - Phys.Rev. C3 (1971), 1137.

(14) W.Glöckle and R.Offermann - Phys. Rev. C16 (1977), 2039.

(15) J.P.Vary and S.N.Yang - Phys.Rev. C15 (1977), 1545

(16) H.N.Comins, Ph.D. Thesis - University of Sidney (1973)

(17) J.C.Sens, F.Rietsch, A.Pape and R.Armbruster - N.P. A199 (1973), 232
J.C.Sens, A.Pape, R.Amsbruster - N.P.A199 (1973), 241
C.Rolfs, A.M.Charlesworth and R.E.Azuma - N.P.A199 (1973), 257
C.Rolfs, W.E.Kieser, R.E.Azuma and A.E.Litherland - N.P. A199 (1973), 274
C.Rolfs, I.Berka, H.P.Trautvetter and R.E.Azuma - N.P.A199 (1973), 328

(18) C.P.Malta and E.A.Sanderson - N.P. A225 (1974), 181
P.J.Ellis and H.A.Mavromatis, N.P.A175 (1971), 309

(19) Walter Glöckle - Private Communication.

TABLE CAPTIONS

TABLE 1 - Parameters of the OBEP. The numbers in brackets are the ratio f/g[11].

TABLE 2 - Deuteron results for the OBEP. The experimental results are given in the first column.

T A B L E 1

		HM1		HM3A		HM3B	
	m_α	g_α^2	Λ_α	g_α^2	Λ_α	g_α^2	Λ_α
π	138.	14.1	2500	14.4	1530	14.4	1265
η	548.5	2.2	2500	6.	1530	6.	1530
ρ	712.	1.4(4.5)	1400	0.77(6.6)	1530	0.77(6.6)	1530
ω	782.8	25.	1300	23.	1530	23.	1530
ϕ	1020.	33.6	1300	5.	1530	5.	1530
σ	550.	5.9	2500	8.2	1530	8.67	1530
δ	960.	8.7	2500	4.99	1530	2.88	1530

T A B L E 2

	Exp.	HM1	HM3A	HM3B
E_b(MeV)	2.22462 ± 0.00006	2.224	2.225	2.223
Q(fm^2)	0.2860 ± 0.0015	0.284	0.281	0.277
P_D(%)	6 ± 2	5.75	5.18	4.70

FIGURE CAPTIONS

Figure 1 - Second order corrections: (a) core polarisation; (b) 4 particles - 2 holes; (c) and (d) Hartree-Fock terms.

Figure 2 - Spectra of ^{18}O as a function of the gap parameter C, for the Reid soft core potential. Dashed lines and full lines correspond to results with base G only and bare plus core polarisation respectively.

Figure 3 - Same as Fig. 1 for HM1.

Figure 4 - Same as Fig. 1 for HM3A.

Figure 5 - Same as Fig. 1 for HM3B.

Figure 6 - Spectra of ^{18}F as a function of C, for the Reid soft core potential. Dashed lines and full lines are the same as in Fig. 1.

Figure 7 - Same as Fig. 5 for HM1.

Figure 8 - Same as Fig. 5 for HM3A.

Figure 9 - Same as Fig. 5 for HM3B.

Figure 10- The ground sate of ^{18}O (bare+core polarisation) as a function of C for all four potentials.

Figure 11- Same as in Fig. 9 for the ground state of ^{18}F.

Figure 12- Spectra of ^{18}O for C=17.5 MeV. Odd columns correspond to bare G-results and even columns to bare plus core polarisation. The last column is the experimental spectrum (only the states identified as two-particle states[17]).

Figure 13 - Same as Fig. 12 for ^{18}F.

Figure 14 - Spectra of ^{18}O for C=12 MeV. The 3rd spectrum shown for the Reid potential contains the two-body effective interaction derived from a three-body potential as explained in the text. The rest is as in Fig. 12.

Figure 15 - Same as Fig. 14 for ^{18}F.

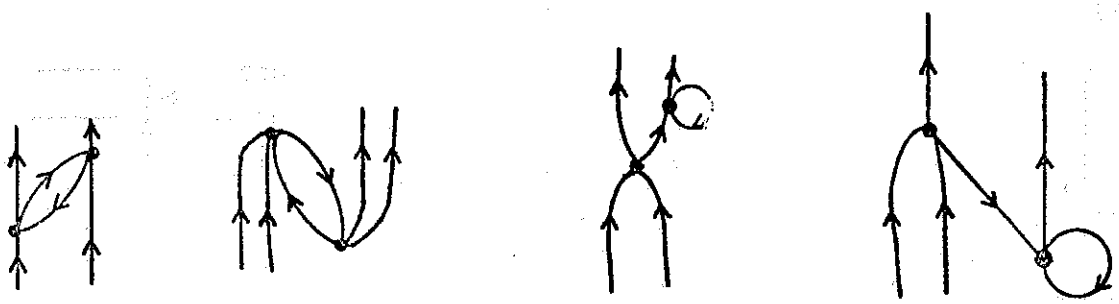

Figure 1

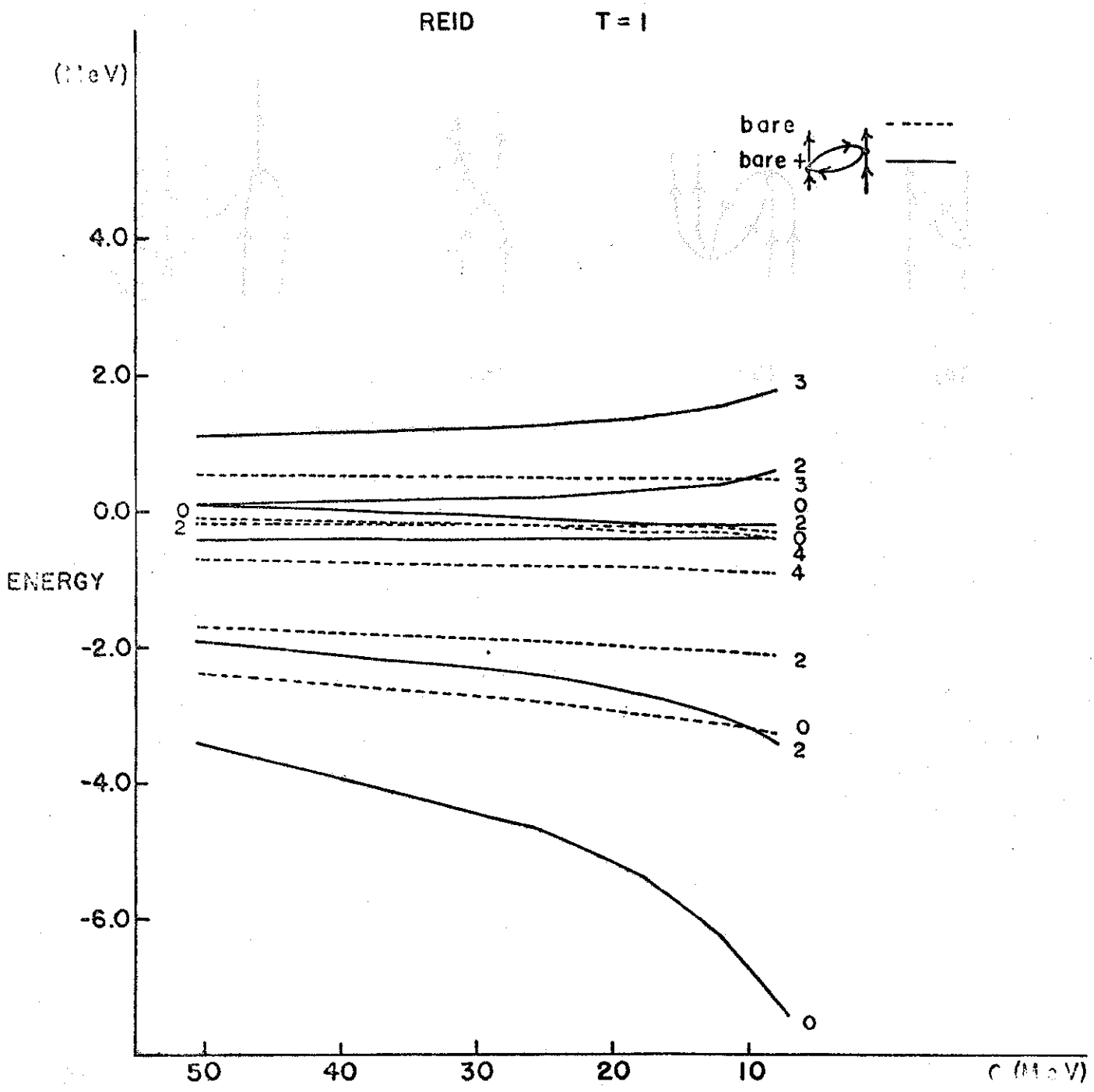
REID
T = 1
bare
bare +
4.0
2.0
0.0
-2.0
-4.0
-6.0
ENERGY
50
40
30
20
10
3
2
3
0
2
0
4
4
2
0
2
0
2
0

Figure 2

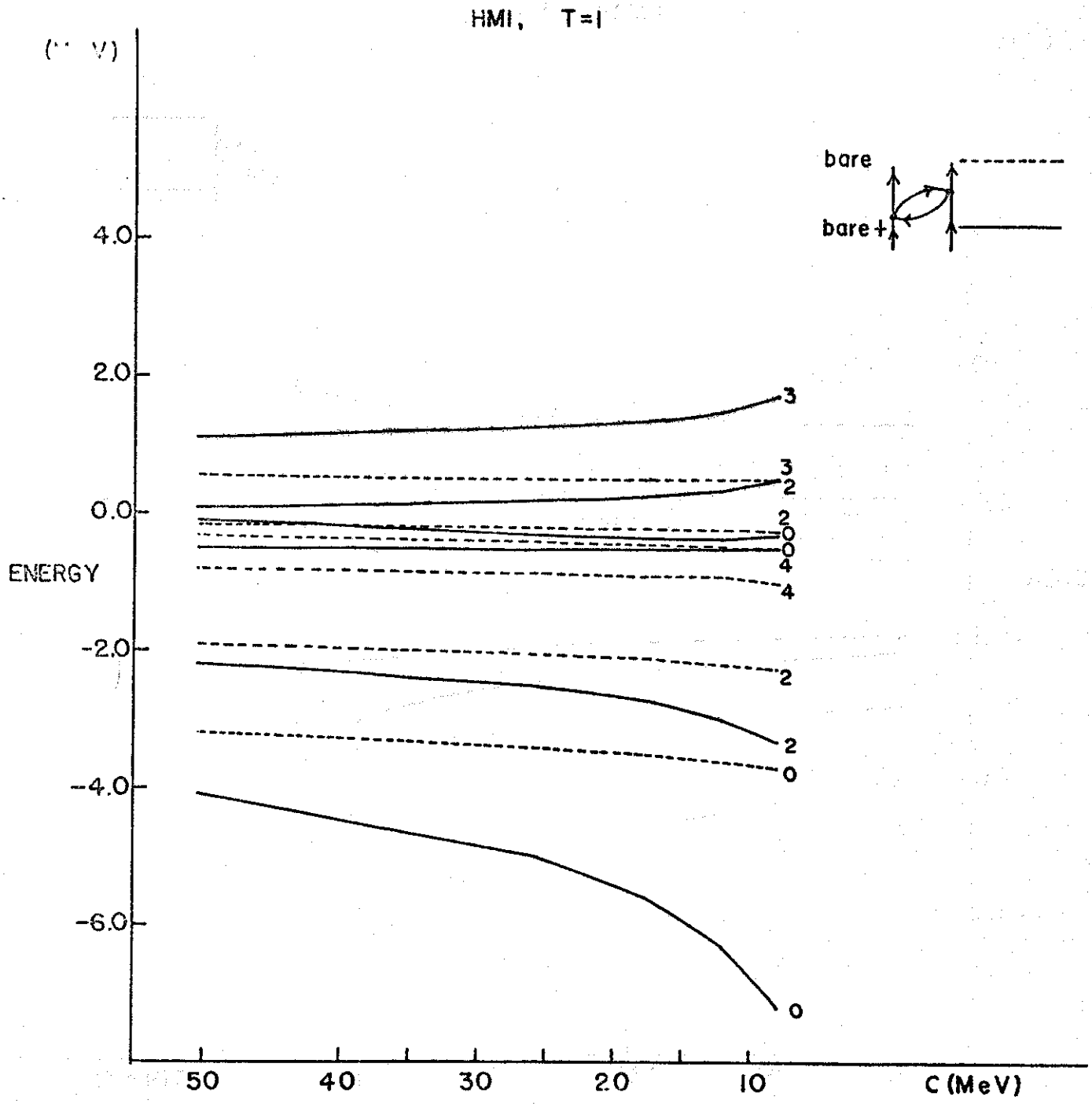
HMI, T=1
bare
bare +
4.0
2.0
0.0
-2.0
-4.0
-6.0
ENERGY
3
3
2
2
0
0
4
4
2
2
0
0
50
40
30
20
10
C (MeV)

Figure 3

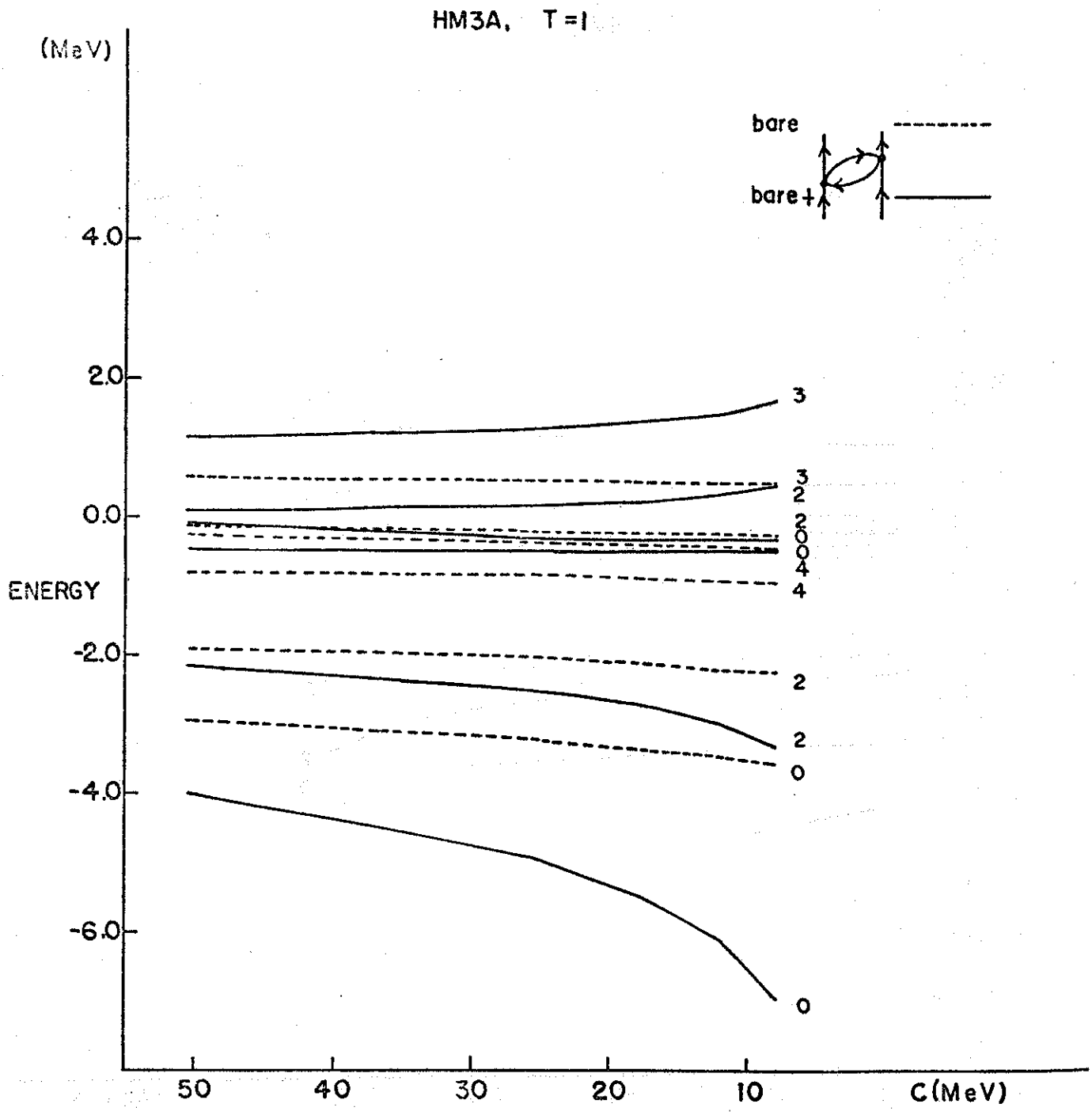
HM3A, T=1
(MeV)
bare
bare +
4.0
2.0
0.0
-2.0
-4.0
-6.0
ENERGY
3
3
2
2
0
4
4
2
2
0
0
50
40
30
20
10
C(MeV)

Figure 4

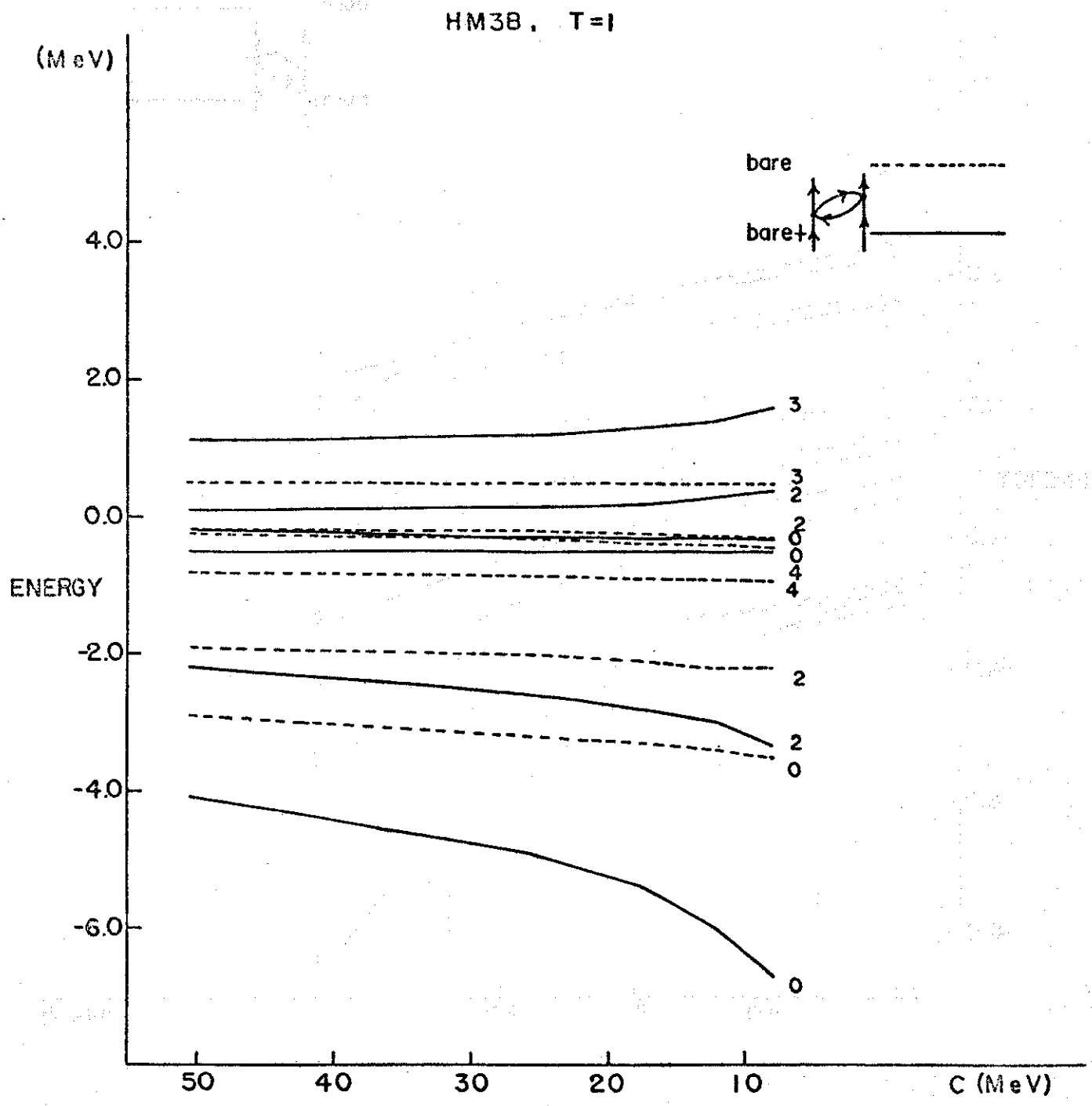
HM38, T=1
(MeV)
bare
bare+
4.0
2.0
0.0
-2.0
-4.0
-6.0
ENERGY
3
3
2
2
0
0
4
4
2
2
0
0
50
40
30
20
10
C (MeV)

Figure 5

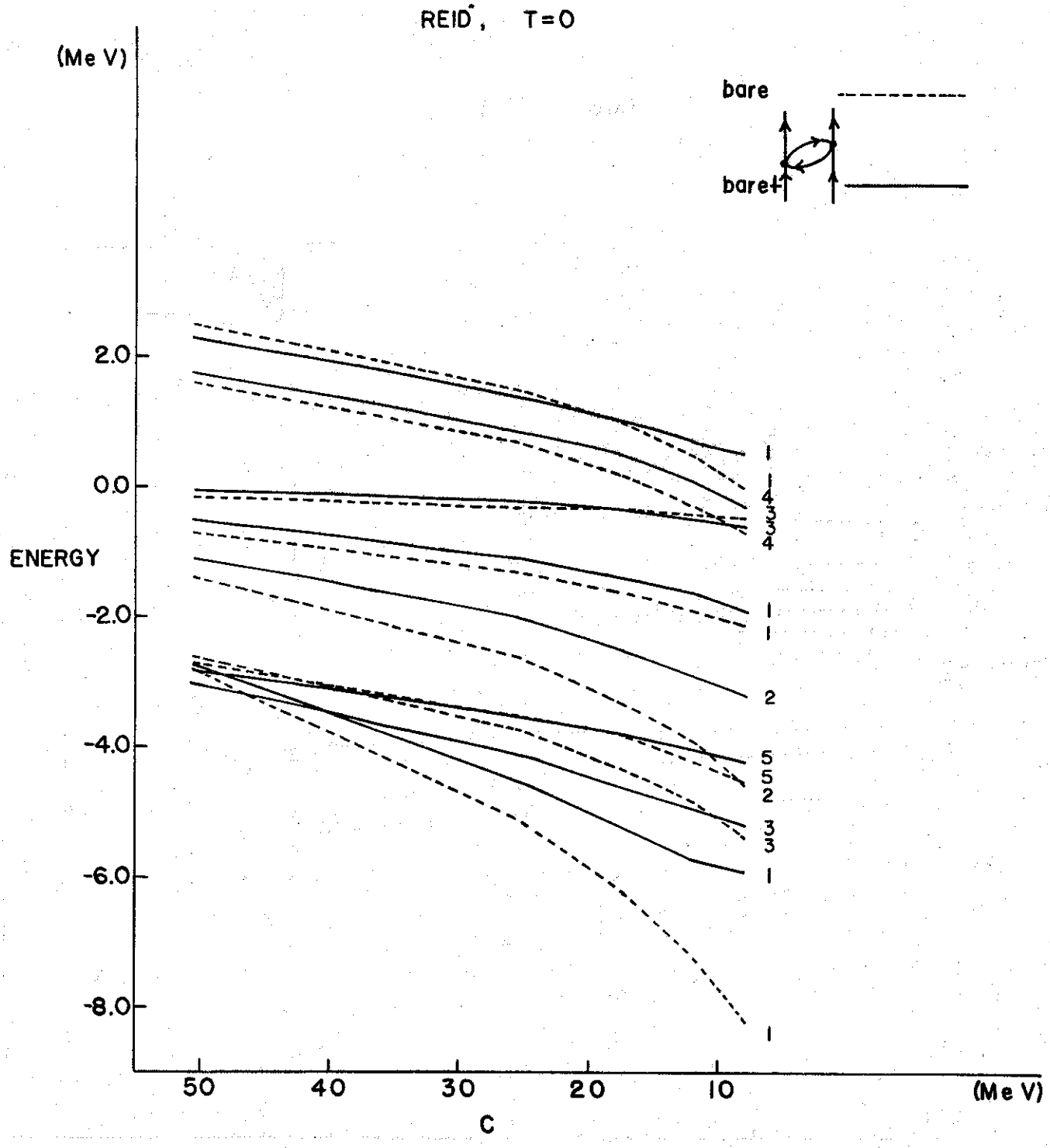
REID*, T=0
(Me V)
bare
bare+
2.0
0.0
ENERGY
-2.0
-4.0
-6.0
-8.0
1
4
4
1
1
2
5
5
2
3
3
1
1
50
40
30
20
10
(Me V)
C

Figure 6

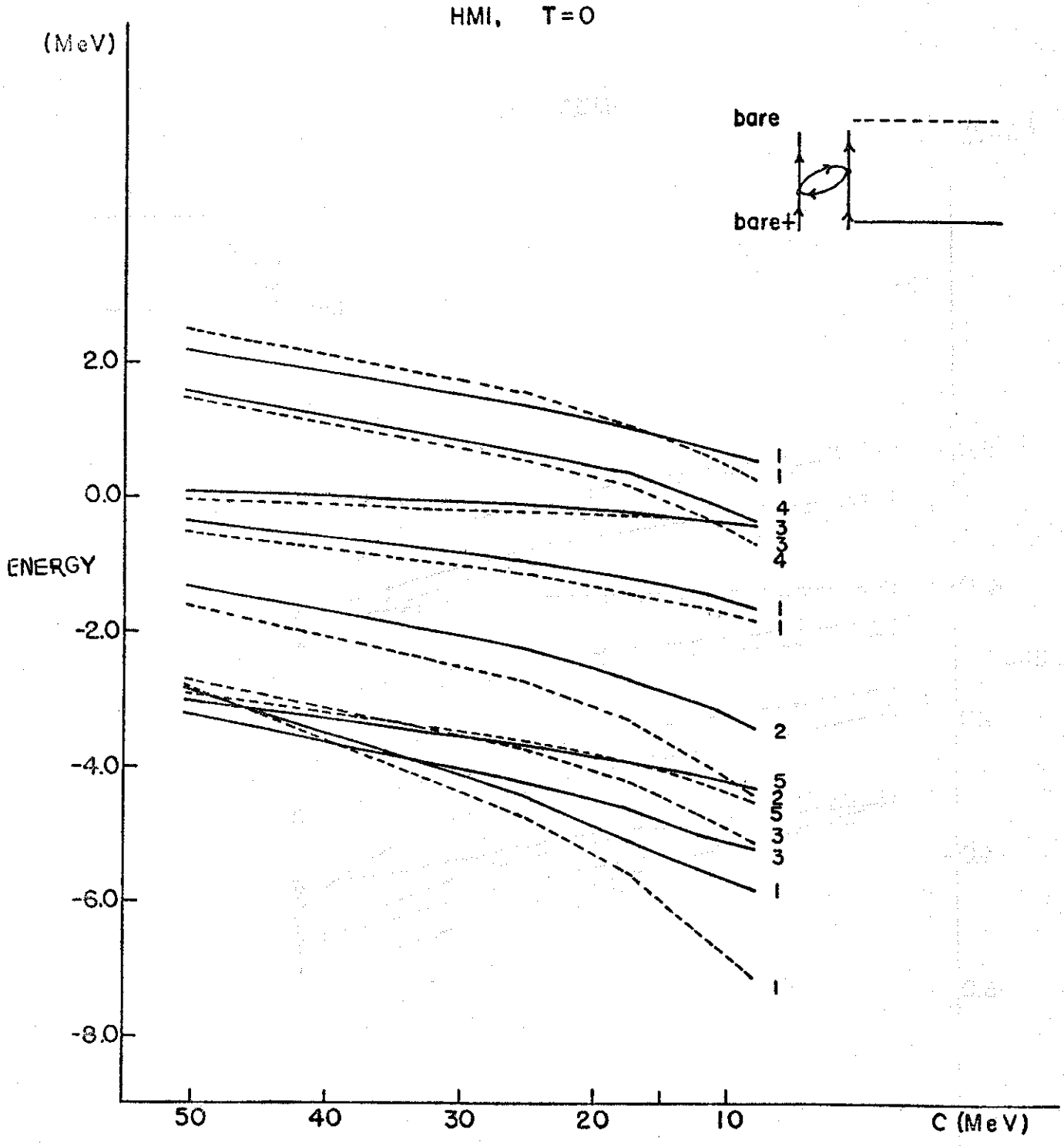

Figure 7

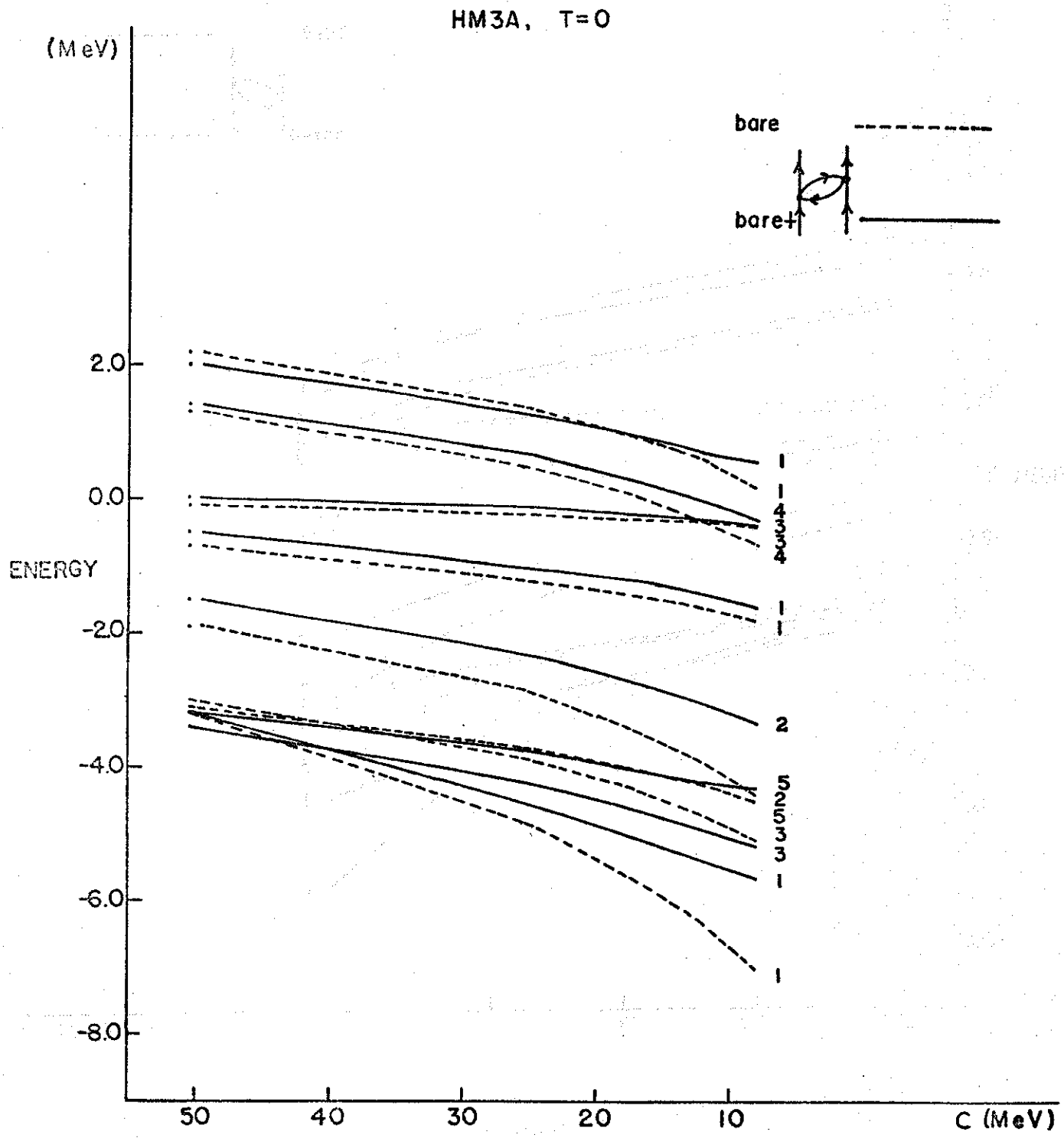
HM3A, T=0
(MeV)
bare
bare+
2.0
0.0
-2.0
-4.0
-6.0
-8.0
ENERGY
1
1
4
3
4
1
1
2
5
5
2
3
3
1
1
50
40
30
20
10
C (MeV)

Figure 8

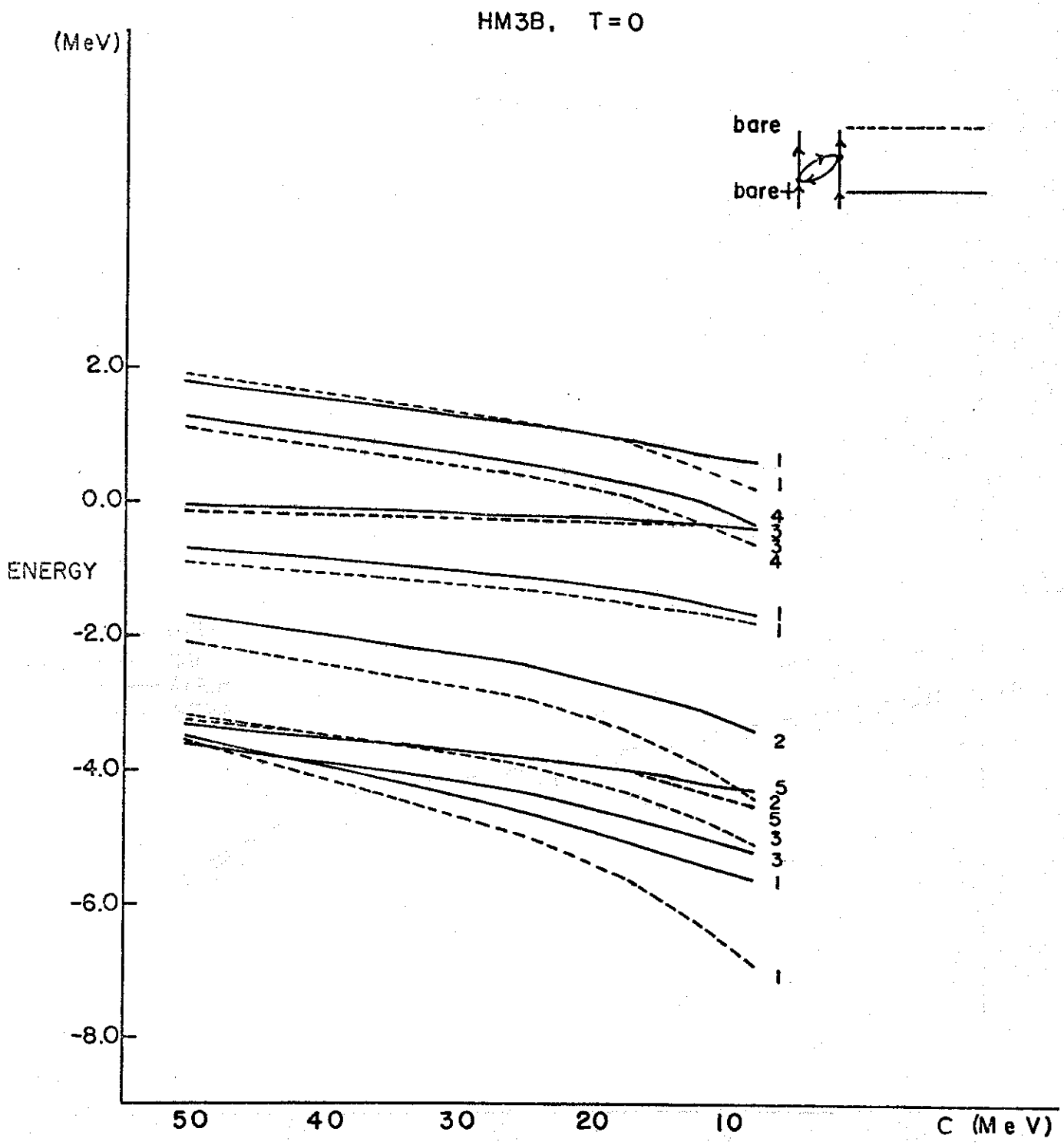
HM3B, T=0
(MeV)
bare
bare+
2.0
0.0
-2.0
-4.0
-6.0
-8.0
ENERGY
1
1
4
4
4
1
1
2
5
5
3
3
1
1
50
40
30
20
10
C (MeV)

Figure 9

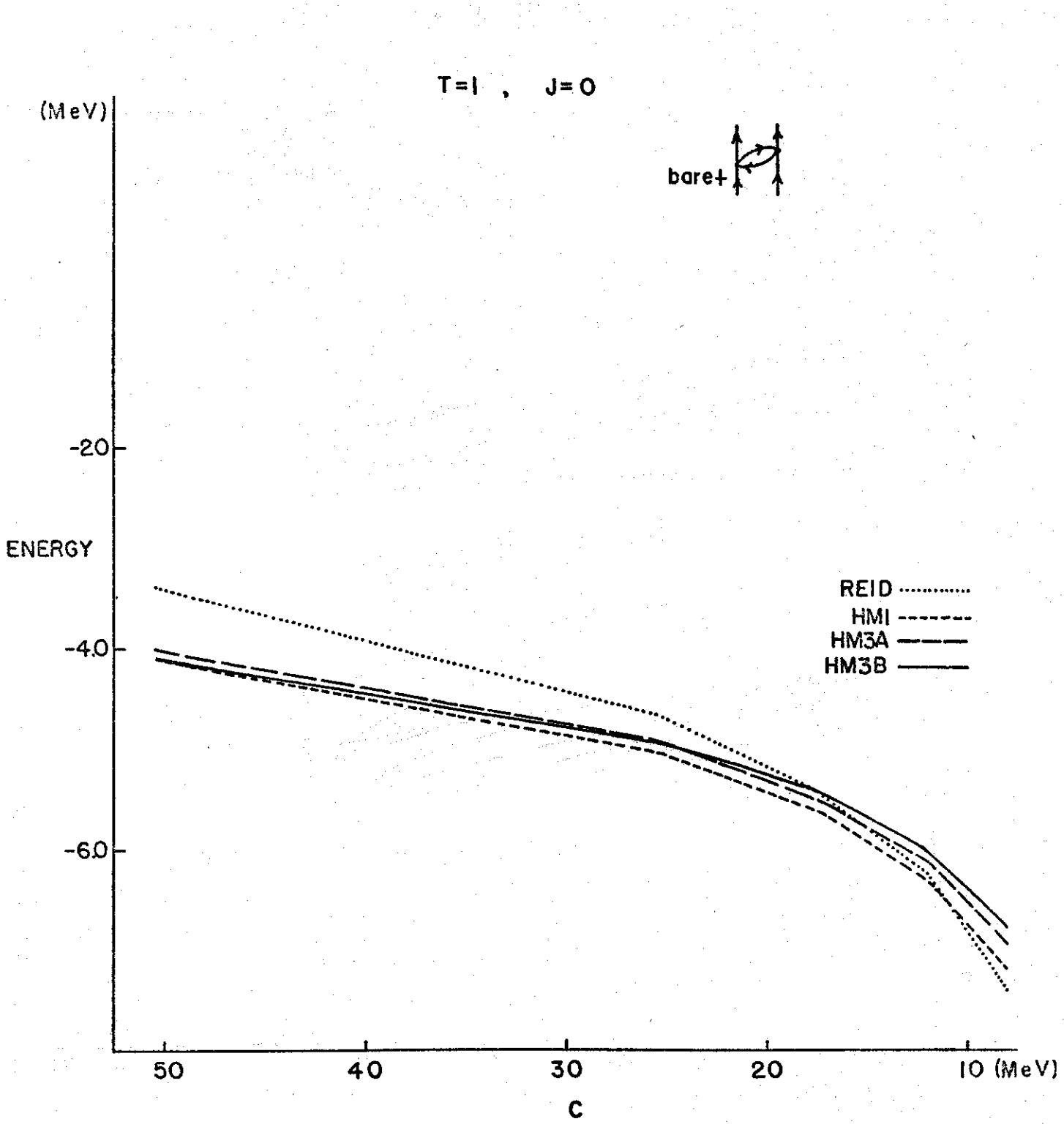
T=1 , J=0
(MeV)
bare+
-20
ENERGY
-40
-60
REID
HMI
HM3A
HM3B
50
40
30
20
10 (MeV)
C

Figure 10

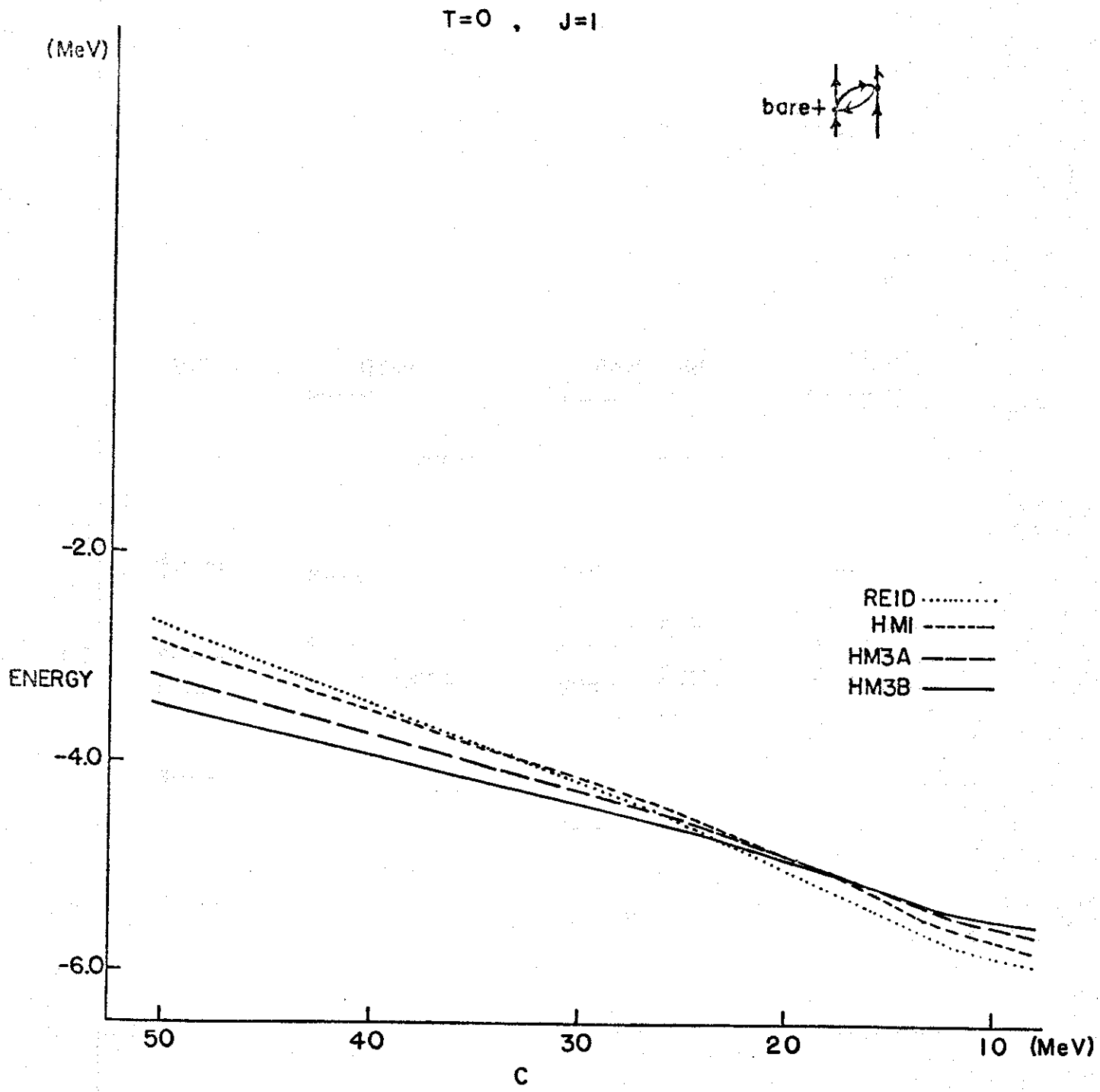
T=0 , J=1
(MeV)
bare+
-2.0
-4.0
-6.0
ENERGY
REID
HMI
HM3A
HM3B
50
40
30
20
10 (MeV)
C

Figure 11

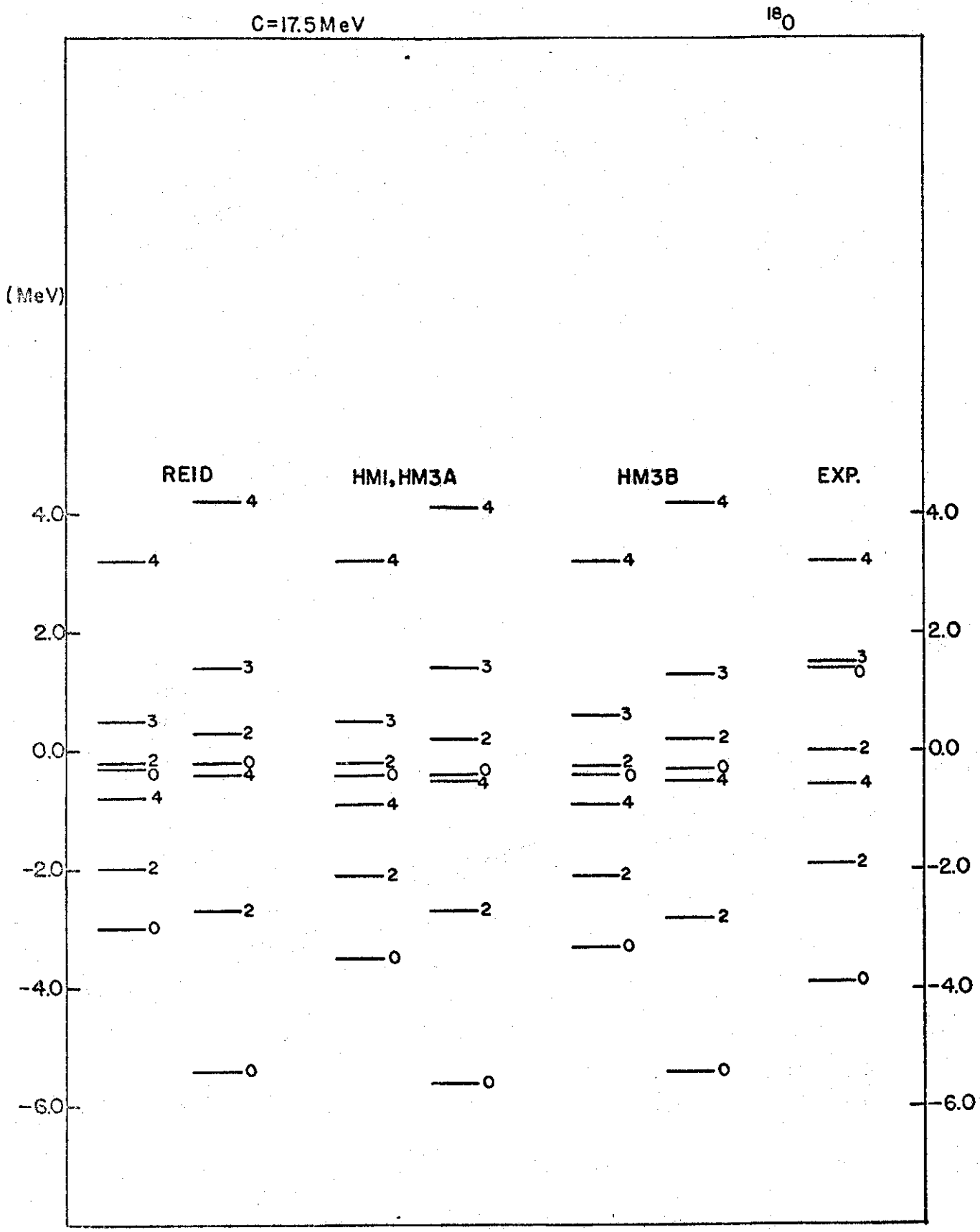

Figure 12

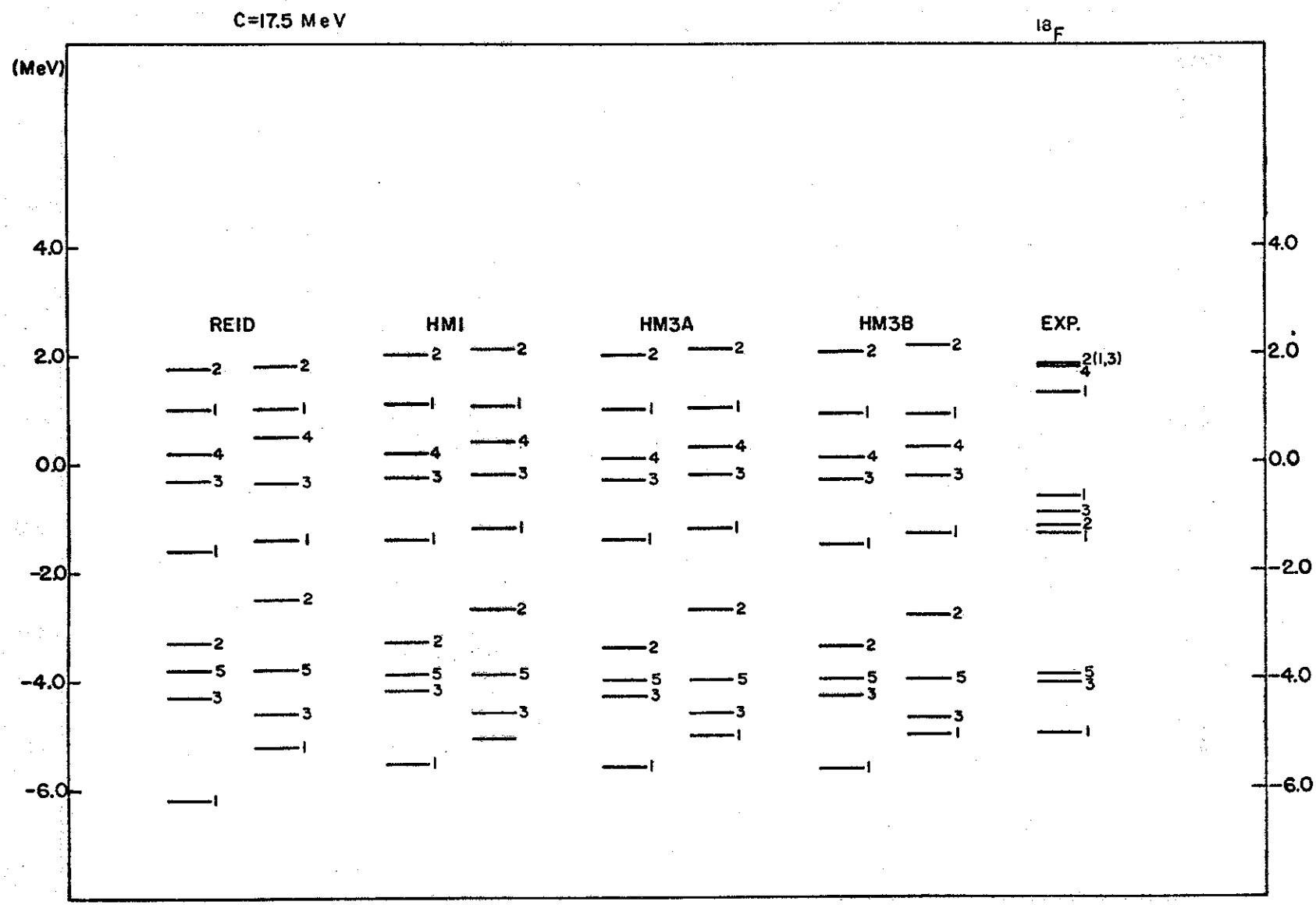

Figure 13

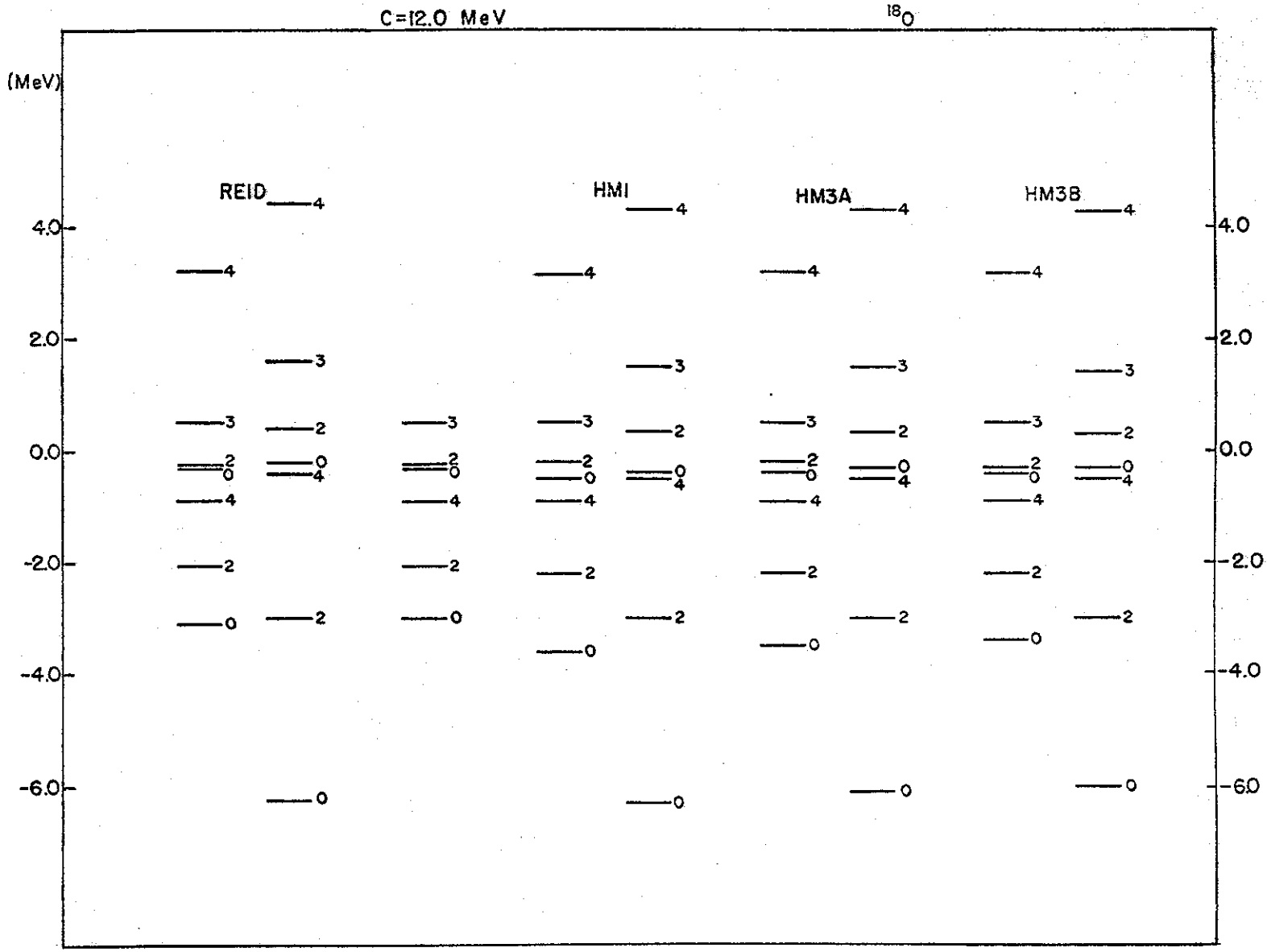

Figure 14

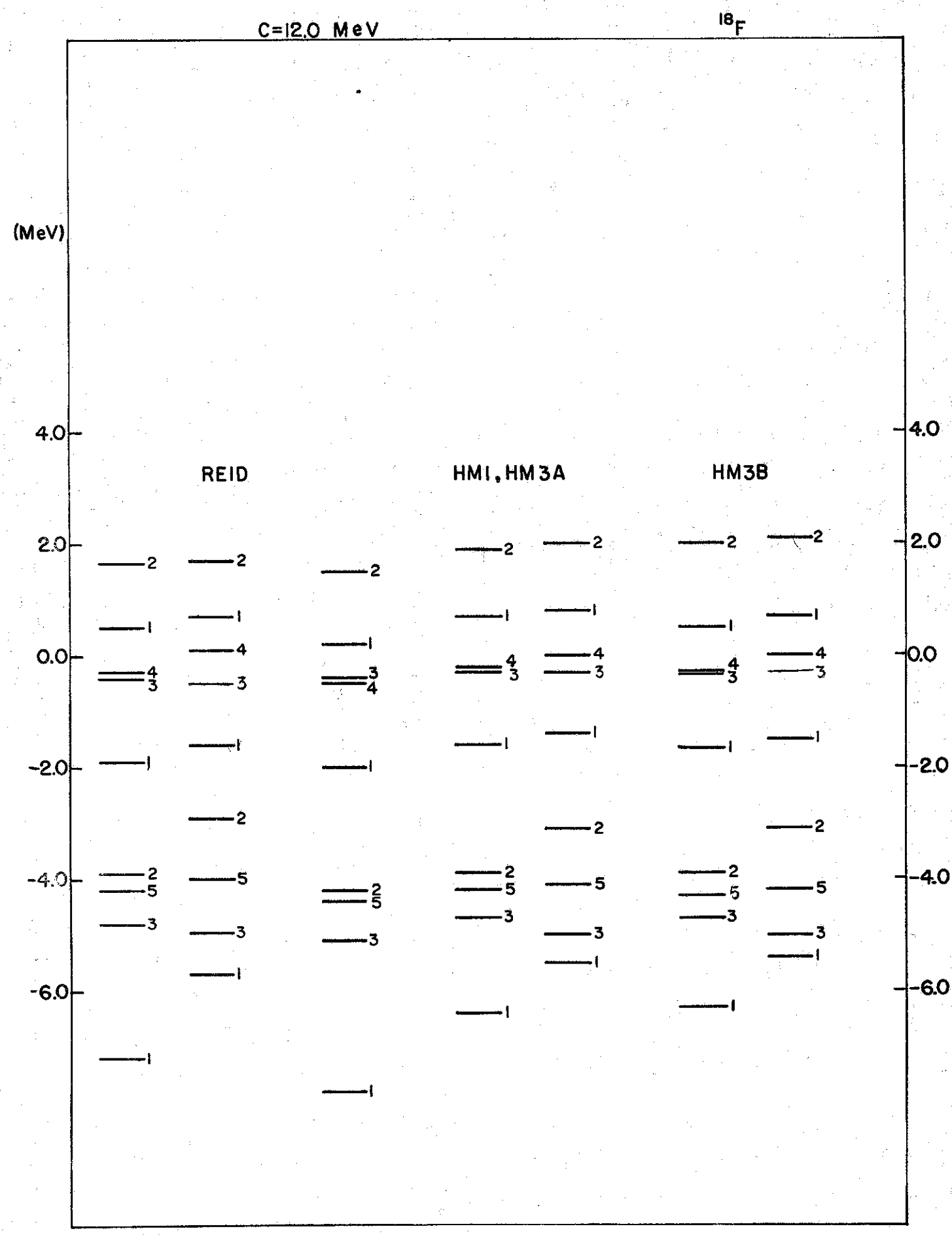

Figure 15